Crystal-to-amorphous transformation of NiTi induced by cold rolling

Crystal-to-amorphous transformation of NiTi induced by cold rolling

J. Koike and D. M. Parkin
Center for Materials Science, Los Alamos National Laboratory, Los Alamos, New Mexico 87545

M. Nastasi
Materials Science and Technology Division, Los Alamos National Laboratory, Los Alamos, New Mexico 87545

(Received 9 March 1990; accepted 23 March 1990)

A NiTi intermetallic compound was cold rolled at room temperature by 30% and 60% thickness reductions, and microstructures were studied by means of transmission electron microscopy (TEM). In the cold-rolled samples we observed both a phase of nanometer-sized crystals and an amorphous phase. A substantially high dislocation density, 10^{13} to $10^{14}/cm^2$, was evident in the transition region between crystalline and amorphous phases. A simple estimate of the elastic energy arising from this dislocation density is of the same order as the crystallization energy, suggesting that dislocation accumulation is a major driving force for amorphization in cold-rolled NiTi.

I. INTRODUCTION

Amorphous materials have been traditionally synthesized by condensing a random structure from a liquid or vapor phase. In the last decade, various solid-state techniques have been developed to produce an amorphous phase from a crystalline phase. A basic premise of the solid-state amorphization is to increase the free energy of the crystalline phase to a state higher than that of the amorphous phase. To prevent the nonequilibrium high-energy crystalline phase from transforming to an equilibrium stable state, amorphization is always carried out at low temperatures where atomic mobility is sufficiently low to prevent diffusion that leads to the equilibrium state. Under this kinetic restriction, the thermodynamic requirement for amorphization can be fulfilled in many intermetallic, ceramic, and semiconductor systems by means of high-energy particle irradiation, hydrogenation, ion-beam mixing, ion implantation, mechanical mixing, and annealing of diffusion couples. For each amorphizing technique, extensive studies have been carried out to understand the thermodynamic driving force and the underlying mechanism.[1]

In Kr-irradiated Zr_3Al, Rehn *et al.*[2] observed chemical disordering, lattice dilation, and a substantial softening of shear modulus before amorphization. They found a linear relation, similar to that seen during heating to the melting point,[3] between the shear modulus and dilation. These results indicate that the onset of amorphization may be triggered by an elastic instability caused by shear-modulus softening associated with lattice dilation and chemical disordering.[2] Similar observations are found in other solid-state amorphization techniques. During hydrogenation of Zr_3Al,[4] a dilation observed before amorphization was identical to that of Kr-irradiated Zr_3Al, indicating that a critical dilation may induce the elastic instability independent of the method. For B implantation into Nb,[5] the mean square displacement of atoms from their lattice site, derived from the measured x-ray diffuse intensity, increases to a large maximum value before amorphization takes place. In this instance, the mean square displacement averaged along the principal crystallographic axes is equivalent to the lattice dilation. It has also been reported that NiTi[6] and GaSb[7] can be amorphized by applying a shear stress under high pressure. These results can be understood in terms of elastic instability caused by the external shear stress instead of the internal stress induced by irradiation or hydrogenation. Consistent with experimental observation, molecular dynamics simulation of amorphization by interstitial insertion[8] and chemical disordering[9] shows a strong correlation between amorphization and an increase in the mean square displacement and dilation, respectively. These results all imply that the mean square displacement of lattice atoms (or equivalently, the lattice dilation) is a key factor underlying solid-state amorphization.[10]

NiTi is known to be susceptible to amorphization under irradiation[11,12] and shear deformation.[6] In the present work, cold rolling was employed in polycrystalline NiTi. As discussed above, amorphization can be expected by cold rolling if a critical amount of atomic displacement is induced. We examined the microstructure of cold-rolled samples using conventional TEM and high-resolution electron microscopy (HREM) techniques. We determined dislocation density from HREM images. We then estimated the elastic energy associated with dislocations and compared it to the

crystallization energy of the amorphous phase. The thermodynamic driving force for amorphization is discussed here based on the obtained results. We also address the crystalline stability under mechanical deformation in terms of dislocation melting theory.[13–15]

II. EXPERIMENTAL

Nearly equiatomic NiTi alloy sheets obtained from RAYCHEM had a composition determined by chemical analysis of Ni–49.2 at.% Ti. Using electron energy loss spectroscopy (EELS), we determined that the local composition was spatially uniform within an error of ±4 at.%. These spectra were used as a standard to determine the ratio of the inelastic scattering cross section of two elements for the composition analysis of cold-rolled samples. TEM examination of as-received material showed the characteristic twin microstructure of the martensite phase. By focusing and defocusing the electron beam with an incident energy of 300 keV, we established a martensite starting temperature slightly above room temperature, as indicated by the disappearance and reappearance of twins, respectively. The alloy sheets (2.5 cm × 1.25 cm × 0.2 cm) were cold rolled at room temperature to thickness reductions of 30% and 60%. During cold rolling, samples were sandwiched between two stainless steel sheets to improve the fracture toughness. The cold-rolled sheets were mechanically ground to ~300 μm. Disks of 3-mm diam were spark-cut and jet-polished with an electrolyte mixture consisting of 5.3 g LiCl, 11.2 g $Mg(ClO_4)_2$, 500 ml methanol, and 100 ml buthyl cellosolve.[16] Microstructure was investigated with a Philips CM-30ST and CM-30STEM, both operated at 300 kV.

III. RESULTS

Bright-field images and selected area diffraction patterns of as-received, 30% cold-rolled, and 60% rolled samples are shown, respectively, in Figs. 1(a), 1(b), and 1(c). The bright-field image of the as-received sample exhibits a twin structure. A number of lattice defects are seen inside the twinned grains, as is usually observed in martensitic NiTi, and the diffraction pattern can be indexed as the monoclinically distorted B19 structure of martensitic NiTi.[17] After 30% reduction [Fig. 1(b)], the bright-field image exhibits a finer twin size than that observed in the as-received sample. The complicated image contrast indicates severe strain in the crystal. The corresponding diffraction pattern exhibits a weak diffuse ring intensity with strong crystalline spots superposed, indicating that a small volume fraction of the amorphous phase is formed by 30% reduction. Further thickness reduction to 60% produces more amorphous volume, as shown in Fig. 1(c). The bright-field image reveals two different contrast regions, denoted as α and x in the figure. The diffraction pattern corresponding to the region α shows only a diffuse ring pattern, indicating the presence of an amorphous structure. The diffraction pattern from the region x shows both crystalline spots and a diffuse ring pattern.

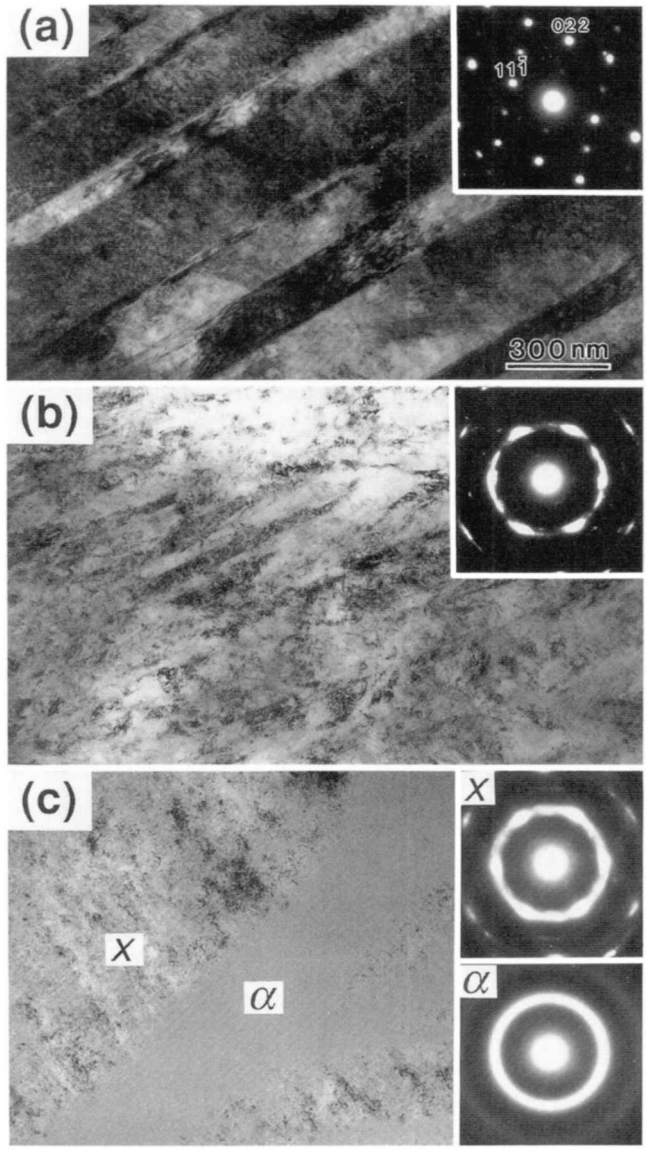

FIG. 1. The bright-field images and the corresponding diffraction patterns of NiTi (a) as-received, (b) 30% reduced, and (c) 60% reduced.

Composition analysis of the 60% reduced sample using EELS shows a local composition variation of ±8 at.% from the original value throughout the sample. A small volume fraction (<5%) of equilibrium precipitates of Ni_3Ti and $NiTi_2$ was also observed and found to be resistant to amorphization. The composition variation occurs presumably because of either enhanced diffusion caused by elastic strain or heating effects encountered during the cold-rolling process.

However, we found no correlation between composition variation and the amorphous phase formation. One may find amorphous phase in areas where the composition is the same as the as-received sample. For instance, the composition taken from the area shown in Fig. 1(c) is found to be Ni–49.4 at. % Ti for both α and x regions.

Using HREM, we further investigated the microstructure of the samples reduced by 30% and 60%. Figure 2 is a typical HREM image of the 30% reduced sample. The image shows two different areas—one defined with clear lattice fringes, indicating a crystalline structure, and the other without lattice fringes, indicating an amorphous structure. Lattice fringes running along the two different directions are (010) and (001) planes in the [101] and [110] zone axes, respectively. This is the same twinning mode observed in the transformation from the parent to the martensite phase.[18]

Figure 3 is an HREM image taken from a different place in the 30% reduced sample, showing a transition area between the crystal and amorphous structure. From lower left to upper right, the figure illustrates lattice fringes that gradually fade away. Because the lattice fringe contrast depends on both the sample thickness (t) and the crystalline orientation, expressed by the deviation parameter from the Bragg angle (s),[19] an investigation of the mechanically induced lattice defects using lattice fringe images is valid only if no variation in these parameters exists. Assuming t and s are constant in the observation area, the local dislocation density in Fig. 3 can be determined by counting lattice fringe termination. This density is about $1 \times 10^{13}/\text{cm}^2$ in the left part of the figure and about $5 \times 10^{13}/\text{cm}^2$ in the upper middle part.

When there is a spatial variation in t by some multiple of $\Delta t = \xi_g/2$ (where ξ_g is the extinction distance, typically a few tens of nm in metals[20]), a corresponding absence of lattice fringes is expected,[19] similar to what

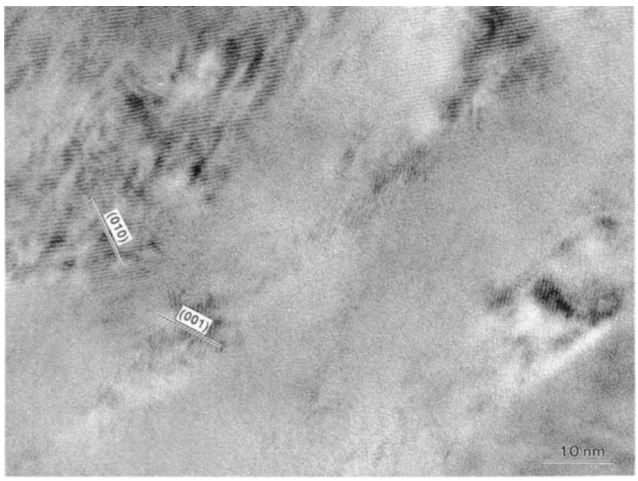

FIG. 2. The lattice fringe image of 30% reduced NiTi.

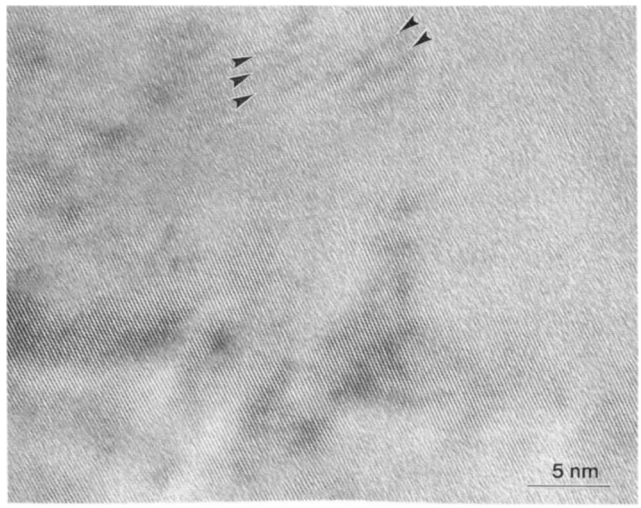

FIG. 3. The lattice fringe image taken from a different area of the same sample shown in Fig. 2.

is seen in the area indicated by arrows. Because the observed periodicity of the fringe absence derived from the distance between arrows is 1 to 2 nm, a drastic variation of the thickness would be required to explain our results. Clearly, this is not the case from the uniform image contrast observed in the figure.

Variation in s may also give rise to a periodic absence of lattice fringes at an interval of $\Delta s = 1/4t$.[19] Assuming t to be a constant 30 nm (a typical TEM sample thickness), a Δs of 1/1200 nm^{-1} corresponds to a tilt of, for example, the (001) plane by 3.8×10^{-3} rad. This tilt yields a difference in the lattice spacing between the top and bottom surfaces of 0.11 nm, 25% of the (001) spacing. Such a difference cannot be accommodated by elastic strain and requires a dislocation production. Taking the periodicity of the fringe absence (1 to 2 nm) as a measure of this dislocation distance, an estimated dislocation density is 2.5×10^{13} to $1 \times 10^{14}/\text{cm}^2$, which is in good agreement with the dislocation density estimated by counting the lattice fringe termination ($5 \times 10^{13}/\text{cm}^2$).

Figure 4 shows an HREM image corresponding to the area x in Fig. (1c). The image exhibits many small crystalline grains with different orientations characterized by lattice fringes running along various directions with various spacings. The grain diameter is >10 nm, a substantially smaller value than that observed in pure metals whose grain diameter saturates at several μm during cold rolling.[21] The lattice fringe image is not clear in the area where two crystals with different orientations meet. This is probably caused by either the formation of an amorphous phase or by multiple grain overlapping effects along the projected direction of the incident electron beam.

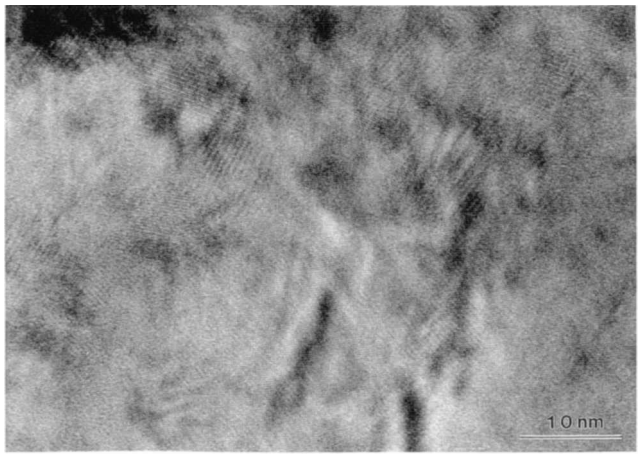

FIG. 4. The lattice fringe image of 60% reduced NiTi, corresponding to the area x in Fig. 1(c).

IV. DISCUSSION

Our present results show the formation of an amorphous phase in cold-rolled NiTi. An extremely high dislocation density of 10^{13} to $10^{14}/cm^2$ is observed in a transition region between the crystalline and amorphous phases, which corresponds to a nearest dislocation distance of 3 to 1 nm, respectively. If dislocations exist closer than this distance, the dislocation cores would begin to overlap, and the crystalline structure cannot be defined. Hence, a dislocation density of about $10^{14}/cm^2$ appears to be the upper limit for crystalline stability.

Jensen *et al.*,[15] using the molecular dynamics calculation, showed that a crystal may exhibit a liquid structure when dislocation density increases. They calculated the pair distribution function $g(r)$ in an fcc crystal as a function of dislocation density at temperatures of 0 K, 1/4 T_M, and 1/2 T_M, where T_M is melting temperature. A significant result of their work was that $g(r)$ looked similar to that of a liquid at dislocation densities greater than 15%, independent of temperature. Assuming a weighted average surface atomic density of Ni and Ti ($1.8 \times 10^{15}/cm^2$), a dislocation density of 15% corresponds to 2.7×10^{14} dislocations/cm^2, which is very close to what we have experimentally observed. Jensen *et al.* also showed an increase of lattice dilation with increasing dislocation density, which would soften the shear modulus based on the Grüneisen relation,[22] consistent with the results reported in Kr-irradiated Zr_3Al.[2]

The energy associated with dislocations can be estimated by using the expression Gb^2, where G is the shear modulus and b is the Burgers vector. Assuming that b is the smallest lattice parameter of the NiTi unit cell (0.289 nm),[17] and that G is equal to that of the parent B2 structure (C_{44} = 35 GPa),[23] an estimated elastic energy is 2.2 kJ/g-atom for a dislocation density of $10^{14}/cm^2$. When the effect of dislocation interaction is taken into account, the total elastic energy will be larger than this value. Buschow[24] measured crystallization energies for the amorphous Ni-Ti alloys, which are 2.95, 3.43, 3.77, and 3.44 kJ/g-atom for Ni–38, –40, –65, and –70 at.% Ti, respectively. Because the crystallization energy of Ni–Ti alloys appears to be weakly dependent on the alloy composition, it would be reasonable to assume that the crystallization energy of NiTi is in this same range. This rough estimate indicates that the elastic energy caused by a dislocation density of $10^{14}/cm^2$ is of the same order as the crystallization energy. Thus, dislocation accumulation appears to be a major component of the driving force for amorphization induced by cold rolling.

In intermetallic compounds, dislocation formation often introduces chemical disordering. In the case of irradiation-induced amorphization, chemical disordering has been suggested to provide a driving force for amorphization.[25] If chemical disordering occurs during cold rolling of NiTi, the total energy increase would be higher than the value estimated from dislocation accumulation alone. However, more extensive analysis of diffraction patterns will be necessary to examine the possibility of chemical disordering in cold-rolled NiTi.

The present results also show that the crystalline size becomes smaller with increasing thickness reduction. The sample reduced by 60% exhibits nanometer-sized crystals, as well as an amorphous phase. Hellstern *et al.*[26] also observed the formation of nanocrystals (5 to 12 nm in diam) in ball-milled NiTi and other B2 compounds; however, an amorphous phase was not observed. They explained that this effect may be caused by an absence of complete chemical disordering, based on the fact that the chemical long-range order parameter remained >0.65 after ball milling. It is also possible to account for the difference between their results and ours in terms of heating effects caused by deformation and temperature-dependent dislocation mobility. Suppose that two types of dislocations, one mobile and the other immobile at room temperature, are formed by both cold rolling and ball milling. Creation of nanocrystals may take place by mobile dislocations forming subgrain boundaries, while amorphization may occur as a result of the accumulation of immobile dislocations. With increasing temperature, the dislocations that are immobile at room temperature eventually become mobile and form nanocrystals instead of an amorphous phase. Shultz *et al.*[27] reported that sample temperatures during ball milling can rise to 200 °C. If this is a sample temperature for Hellstern's experiment, both types of dislocations may be mobile and the formation of nanocrystals would result. In contrast to the ball-milling process, typical sample temperatures en-

countered during cold rolling have been reported to be lower than 40 °C.[28] Thus, during cold rolling, the probability of dislocation accumulation is higher than ball milling, and amorphization can result.

V. CONCLUSION

An amorphous phase was partially formed in NiTi during cold rolling to 60% at room temperature. An extremely high dislocation density (10^{13} to 10^{14}/cm^2) was observed in the transition region between the crystal and amorphous phases. A simple estimate of the elastic energy caused by this dislocation accumulation was found to be the same order of magnitude as the crystallization energy. Thus, the accumulation of dislocations appears to be a major component of the driving force for amorphization in cold-rolled NiTi.

ACKNOWLEDGMENT

This work was performed under the auspices of the United States Department of Energy.

REFERENCES

[1]See, for example, J. Less-Common Metals **140** (1988) (Proc. of the 1st Int. Conf. on the Solid-State Amorphizing Transformation, edited by R. Schwarz and W. L. Johnson).
[2]L. E. Rehn, P. R. Okamoto, J. Pearson, R. Bhadra, and M. Grimsditch, Phys. Rev. Lett. **59**, 2987 (1987).
[3]J. L. Tallon, Philos. Mag. A **39**, 151 (1979).
[4]W. J. Meng, P. R. Okamoto, B. J. Kestel, L. J. Thompson, and L. E. Rehn, Appl. Phys. Lett. **53**, 1820 (1988).
[5]G. Linker, Vacuum **36**, 493 (1986).
[6]YE V. Tat'yanin, V. G. Kurdyumov, and V. B. Fedrov, Fiz. Metal. Metalloved. **62**, 133 (1986).
[7]M. M. Aleksandrova, V. D. Blank, A. E. Golobokov, YU. S. Koyaev, A. YU. Zerr, and E. I. Estrin, Phys. Status Solidi A **105**, K29 (1988).
[8]H. Hsieh and S. Yip, Phys. Rev. B **39**, 7476 (1989).
[9]C. Massobrio, V. Pontikis, and G. Martin, Phys. Rev. Lett. **62**, 1142 (1989).
[10]J. Koike, P. R. Okamoto, L. E. Rehn, R. Bhadra, M. Grimsditch, and M. Meshii (Proc. Mater. Res. Soc. Symp.) (Materials Research Society, Pittsburgh, PA, 1990), Vol. 157, p. 777.
[11]J. L. Brimhal, H. E. Kissinger, and A. R. Pelton, Rad. Effects **90**, 241 (1985).
[12]G. Thomas, H. Mori, H. Fujita, and R. Sinclair, Scripta Metall. **16**, 589 (1982).
[13]S. Mizushima, J. Phys. Soc. Jpn. **15**, 70 (1960).
[14]D. Kuhlmann-Wilsdorf, Phys. Rev. **140**, A1599 (1965).
[15]E. J. Jensen, W. Damgaard Kristensen, and R. M. J. Cotterill, Philos. Mag. **27**, 623 (1973).
[16]B. J. Kestel, Ultramicroscopy **19**, 205 (1986).
[17]K. Otsuka, T. Sawamura, and K. Shimizu, Phys. Status Solidi A **5**, 457 (1971).
[18]K. M. Knowles, Philos. Mag. A **45**, 357 (1982).
[19]H. Hashimoto, M. Mannami, and T. Naiki, Philos. Trans. A **253**, 459 (1961).
[20]P. Hirsch, A. Howie, R. B. Nicholson, D.W. Pashley, and M. J. Whelan, in *Electron Microscopy of Thin Crystals* (Robert E. Krieger Pub. Co., Malabar, FL, 1977), 2nd ed., p. 510.
[21]P. Cotterill and P. R. Mould, in *Recrystallization and Grain Growth in Metals* (Halsted Press, New York, 1976), p. 10.
[22]E. Grüneisen, in *Handbuch der Physik* (Julian Springer, Berlin, 1926), Vol. 10, p. 1.
[23]O. Mercier, K. N. Melton, G. Gremaud, and J. Hagi, J. Appl. Phys. **51**, 1833 (1980).
[24]K. H. J. Buschow, J. Phys. F: Met. Phys. **13**, 563 (1983).
[25]D. E. Luzzi, H. Mori, H. Fujita, and M. Meshii, Acta Metall. **34**, 629 (1986).
[26]E. Hellstern, H. J. Fecht, Z. Fu, and W. L. Johnson, J. Mater. Res. **4** (6), 1292 (1989).
[27]R. Shultz, M. Trudeau, J. Y. Huot, and A. Van Neste, Phys. Rev. Lett. **62**, 2849 (1989).
[28]M. Atzmon, K. M. Unruh, and W. L. Johnson, J. Appl. Phys. **58**, 3865 (1985).